Thermal stability of differently rolled pure tungsten plates in the temperature range from 1125°C to 1250°C

Larsen, Thomas; Chmelar, Kevin; Larsen, Benjamin Lindegren; Nagy, Patrik; Wang, Kang; Pantleon, Wolfgang

Published in:
Fusion Engineering and Design

Link to article, DOI:
10.1016/j.fusengdes.2023.113581

Publication date:
2023

Document Version
Publisher's PDF, also known as Version of record

Fusion Engineering and Design 192 (2023) 113581

Contents lists available at ScienceDirect

Fusion Engineering and Design

journal homepage: www.elsevier.com/locate/fusengdes

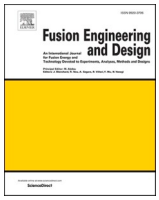

Thermal stability of differently rolled pure tungsten plates in the temperature range from 1125 °C to 1250 °C

Thomas Larsen [a], Kevin Chmelar [a], Benjamin Lindegren Larsen [a], Patrik Nagy [a], Kang Wang [a,b], Wolfgang Pantleon [a,*]

[a] Department of Civil and Mechanical Engineering, Technical University of Denmark, 2800 Kongens Lyngby, Denmark
[b] Institute of Industry and Equipment Technology, Hefei University of Technology, Hefei 230009, PR China

ARTICLE INFO

Keywords:
Tungsten
Plasma-facing material
Annealing
Thermal stability
Recrystallization
Activation energy

ABSTRACT

Application of rolled tungsten as armor of plasma-facing components in future fusion reactors requires its deformation-induced microstructure remaining stable during operation. At high operation temperatures, restoration processes as recovery, recrystallization and grain growth will unavoidably embrittle ductile tungsten achieved by rolling. Three pure tungsten plates manufactured by unidirectional rolling or cross-rolling in two different manners were qualified as baseline material for DEMO. To investigate their thermal stability, hardness testing is performed after isothermal annealing in the temperature range between 1125 °C to 1250 °C. The recrystallization kinetics of the different plates (and different regions within them) is analyzed thoroughly to allow extrapolation outside the investigated temperature range. Significant differences between the recrystallization kinetics of the three tungsten plates originate from the microstructure established by rolling. Two of the plates showed pronounced local differences in their recrystallization kinetics with the core of the plates recrystallizing ahead of the edge regions closest to the rolls. The third plate exhibits best thermal stability without notable differences between the local recrystallization kinetics. Where the two former plates may survive operation for two full power years only at temperatures less than 1005 °C, the later plate could sustain 1035 °C for the same period.

1. Introduction

Tungsten is chosen as armor material for plasma-facing components for future fusion reactors as ITER [1] and DEMO [2] despite its intrinsic brittleness at low temperatures in view of its otherwise superior properties [3,4]. Depending on its microstructure, tungsten behaves ductile at high temperatures and plastic deformation reduces its brittle-to-ductile transition temperature due to structural refinement [3]. Ductility of tungsten at temperatures as low as room temperature is gained by strong plastic deformation [5–7]. The deformation-induced microstructure facilitating the ductile behavior becomes unstable at high temperatures. Thermally activated restoration processes as recovery, recrystallization and grain growth remove the deformation structure and reinstate the brittleness of undeformed tungsten. The restoration kinetics at high temperatures depends strongly on the local microstructure induced by thermo-mechanical processing during manufacturing. Three differently rolled tungsten plates are investigated and their restoration kinetics quantified to predict their maximum operation temperature as armor of a divertor. Potential heterogeneities between different regions within the plates are traced.

2. Material and methods

Rolled tungsten plates are selected as baseline material for plasma-facing components, in particular the divertor, within the work package on materials (WPMAT) of the EUROfusion consortium and characterized by different member institutions [2]. Three different tungsten plates with purity 99.99% complying with the material specifications for ITER were manufactured by A.L.M.T. Corp., Japan (cf. [8]). One plate (termed IGW) was processed by unidirectional rolling, while the other two (designated CLW and CHW) were cross-rolled in two different manners, i.e. the rolling direction was changed by 90° after achieving a certain plate thickness. Further details about the rolling schedule and the initial plate thickness are not revealed [8]. After cutting and

* Corresponding author.
E-mail address: pawo@dtu.dk (W. Pantleon).

https://doi.org/10.1016/j.fusengdes.2023.113581
Received 12 October 2022; Received in revised form 18 January 2023; Accepted 15 February 2023
Available online 28 February 2023

machining, all three manufactured plates have the same sizes of 230×225×12 mm^3 along the (final) rolling direction, transversal direction and normal direction (RD x TD x ND). Two bars of size 5 × 225×12 mm^3 from each plate were received cut along TD by Research Center Jülich from the center of the plates with respect to RD (see the sketch in Fig. 1). Microstructural investigations of the as-received condition revealed certain heterogeneity across the thickness of the plates with respect to grain size and texture and will be discussed elsewhere. Investigation of their thermal stability followed established procedures [9–13].

Small specimens with sizes of 5 × 4 × 5.75 mm^3 along RD, TD, and ND, respectively, are cut from the bars for subsequent annealing treatments. Small fiducial marks introduced on the edges of the specimens allow their distinction. For protection against oxidation and formation of volatile WO_3 during annealing, three cut specimens (each from a different plate) are encapsulated together in a quartz glass ampoule. The ampoules are evacuated, flushed with argon (with purity higher than 99.999%), evacuated again and sealed with a blowtorch. In case an additional annealing condition is required for a specific plate, a single specimen is encapsulated and annealed alone. Specimens in their ampoules are put in a pre-heated ceramic tube furnace NaberTherm RHTC 80/230/15 or NaberTherm RHTH 50/150/18, removed after the desired annealing time and cooled to room temperature by air-cooling.

In order to establish the restoration kinetics of the plates, isothermal annealing treatments are performed at six different temperatures 1125 °C, 1150 °C, 1175 °C, 1200 °C, 1225 °C, and 1250 °C for times up to 1008 h. For each desired annealing time, a separate specimen is annealed at the desired temperature without interruption.

After annealing, macro hardness is determined for the annealed specimens on TD/ND surfaces using a Struers DuraScan 70 hardness tester. A diamond Vickers indenter is applied with a load of 10 kgf and removed after a dwell time of 10 s. A minimum distance of 600 µm between individual hardness indents and between the indents and the specimen surface is ensured to comply with ASTM E92–17 [14]. In view of an observed microstructural heterogeneity in the as-received condition, the hardness after annealing is determined not only in the core of the plates, but additionally close to their edges. Two sets of 12 Vickers indents are placed on the TD/ND surface: one in the edge region (closest to the surface in contact with the rolls during the roiling process), the other in the core region in order to trace through-thickness variations. All indents are inspected optically and unsuitable indents are eliminated. For each set of twelve hardness values, the two extreme values are discarded and the average value of the remaining reported as well as the standard deviation of their average.

The macro hardness of all plates in their as-received state summarized in Table 1 is rather homogeneous throughout the plates with marginally harder cores than edges. The CLW plate is slightly softer than the two others, IGW and CHW.

3. Results

Fig. 2 illustrates the evolution of the macro hardness of the IGW plate

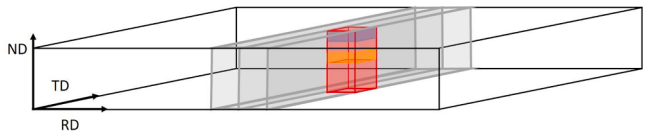

Fig. 1. Sketch of the rolled tungsten plates (black) manufactured by A.L.M.T. illustrating the received bars (gray) cut along TD as well as the cutting of two individual specimens (red) on top of each other for annealing. The two different investigated regions termed core and edge are marked in yellow and blue, respectively, on a TD/ND as well as a RD/ND section of the upper specimen cut for annealing. The coordinate system indicates the final rolling, transversal and normal directions (RD, TD, and ND).

Table 1
Activation energies for two characteristic processes (i) half hardness loss and (ii) half recrystallization together with extrapolated operation temperatures for which half hardness loss or half recrystallization is expected after 2 full power years (fpy). The hardness of the as-received condition of the plates received from A.L.M.T. is added for convenience.

		IGW edge	IGW core	CLW edge	CLW core	CHW edge	CHW core
As-received hardness	HV / HV10	432 ±4	437 ±2	425 ±2	428 ±3	432 ±2	434 ±2
Half hardness loss	Q / kJ/mol	468	472	517	503	464	524
	T(2 fpy) / °C	999	979	1040	1037	991	998
Half recrystallization	Q / kJ/mol	483	499	516	503	480	518
	T(2 fpy) / °C	1004	991	1040	1037	997	995

during annealing at six different temperatures. All hardness curves show progressive softening with annealing time: The hardness decreases from the high value of the deformed state $HV_{def,0}$ of about 435 HV10 in average to the lower value HV_{rex} of about 354 HV10 characteristic for the recrystallized tungsten plates. For short times, the hardness evolution is dominated by recovery, in particular obvious at lower temperatures. In some cases (e.g. edge and core at 1175 °C in Fig. 2c), initial recovery and subsequent recrystallization can be clearly distinguished from their characteristic hardness evolution: a hardness loss with continuously decreasing rate in case of recovery vs. the characteristic softening behavior including a turning point for recrystallization. The significant variation between the hardness values determined on individual specimens for each annealing condition obscures such a distinction in other cases. The higher the temperature, the earlier the onset of the characteristic hardness drop caused by recrystallization with its turning point along the curve is observed. Comparing the different kinetics in Fig. 2 for the different regions reveals that the core of the IGW plate (shown in red) loses its hardness always faster than the edge region (displayed in magenta).

Figs. 3 and 4 present the macro hardness evolution of the two cross-rolled plates, CLW and CHW, respectively. Where the CHW plate (Fig. 4) behaves quite similar to the IGW plate, with almost the same time dependence and its core (shown in blue) recrystallizing significantly faster than its edge (displayed in cyan), the restoration of the CLW plate displays an entirely different behavior: For this plate, almost no differences between core and edge are traced. Additionally, its overall kinetics is much slower than that of IGW and CHW. At low temperatures, a rather abrupt hardness loss due to recrystallization is observed for CLW indicating long periods of incubation before the onset of recrystallization. In these cases, the incubation time dominates the time to achieve a certain progress of recrystallization. During annealing of CLW at 1150 °C, no such hardness drop is observed at all, not even for the specimen annealed for 840 h. The investigations would have to be repeated for a different specimen to account for potential heterogeneities in the plate and continued beyond five weeks to clarify the occurrence of recrystallization at this annealing temperature. In all other cases, recrystallization is observed for all three plates in the entire investigated temperature range from 1125 °C to 1250 °C well below the often quoted recrystallization temperature of 1300 °C (e.g. [2]) due to the long periods of annealing investigated (compare the discussion in [15]).

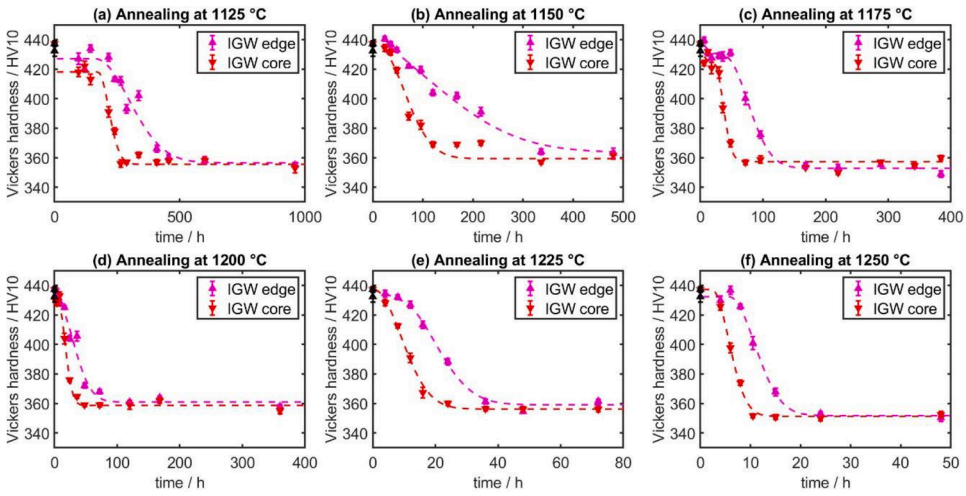

Fig. 2. Hardness evolution in core and edge regions of unidirectionally rolled tungsten plate IGW received from A.L.M.T. during annealing at six different temperatures: (a) 1125 °C, (b) 1150 °C, (c) 1175 °C, (d) 1200 °C, (e) 1225 °C and (f) 1250 °C. The black data points represent the hardness in the as-received condition. The dashed lines present the obtained description of the restoration kinetics by Eqs. (1) and (2).

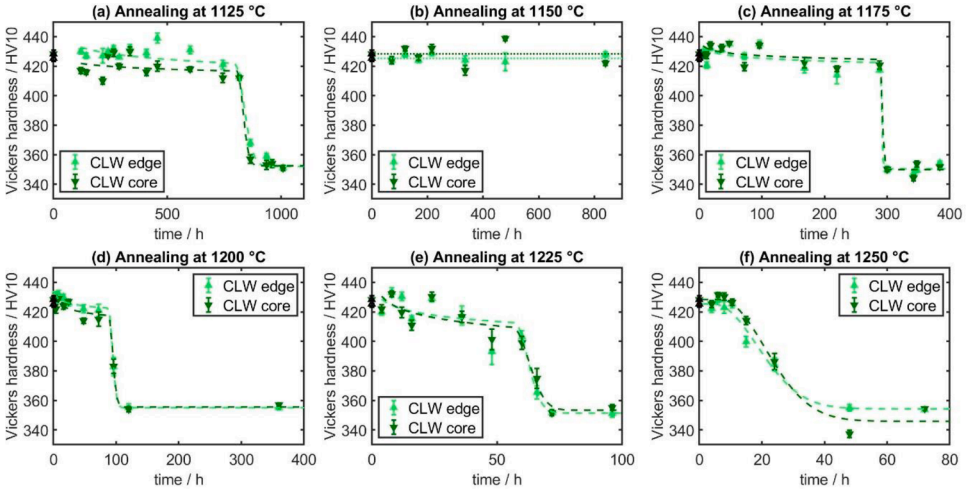

Fig. 3. Hardness evolution in core and edge regions of cross-rolled tungsten plate CLW received from A.L.M.T. during annealing at six different temperatures: (a) 1125 °C, (b) 1150 °C, (c) 1175 °C, (d) 1200 °C, (e) 1225 °C and (f) 1250 °C. The black data points represent the hardness in the as-received condition. The dashed lines present the obtained description of the restoration kinetics by Eqs. (1) and (2). No recrystallization is observed for annealing at 1150 °C as indicated by the dotted lines in (b).

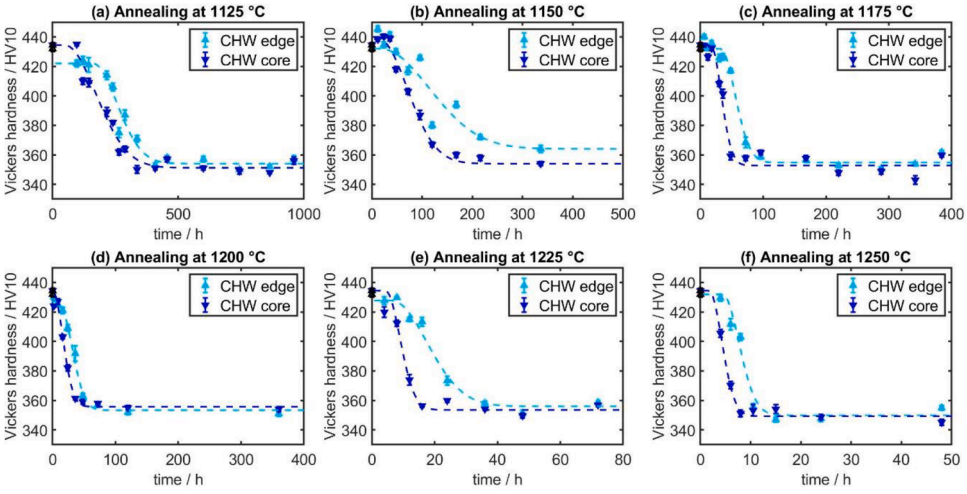

Fig. 4. Hardness evolution in core and edge regions of differently cross-rolled tungsten plate CHW received from A.L.M.T. during annealing at six different temperatures: (a) 1125 °C, (b) 1150 °C, (c) 1175 °C, (d) 1200 °C, (e) 1225 °C and (f) 1250 °C. The black data points represent the hardness in the as-received condition. The dashed lines present the obtained description of the restoration kinetics by Eqs. (1) and (2).

4. Discussion

4.1. Restoration kinetics

For a quantitative analysis of the restoration kinetics, two different characteristic times are considered:

(i) the time to half hardness loss $t_{\Delta HV/2}$, i.e. the time at which the material has lost half of the hardness excess ΔHV above the recrystallized value HV_{rex} and has attained the average value $(HV_{def,0}+HV_{rex})/2$, and
(ii) the time to half recrystallization $t_{X=0.5}$, i.e. the time for which half of the material volume has undergone recrystallization.

Where the former is a heuristic measure straightforwardly accessible for quantifying the overall thermal stability by interpolation, but describing the effect of recovery and recrystallization in a combined manner, the latter enables further insight in the occurring recrystallization process.

For obtaining the time to half recrystallization $t_{X=0.5}$, the measured macro hardness

$$HV = XHV_{rex} + (1-X)HV_{rec} \quad (1)$$

is considered as volume-weighted average between the hardness of the recrystallized regions (HV_{rex}) and that of the deformed and recovered regions (HV_{rec}) with their respective volume fractions X and (1-X). During recovery, the hardness $HV_{rec}(t)$ of the revering regions decreases logarithmically in time [16] (if such a decay is not resolvable from the data, a constant value HV_{rec} is assumed). The recrystallized volume fraction is considered to follow a Johnson-Mehl-Avrami-Kolmogoroff [17] kinetics

$$X = 1 - \exp(-b^n(t-t_{inc})^n) \quad (2)$$

with an incubation time t_{inc} (e.g. [9]), an Avrami exponent n and a rate coefficient b characterizing nucleation and growth of recrystallized

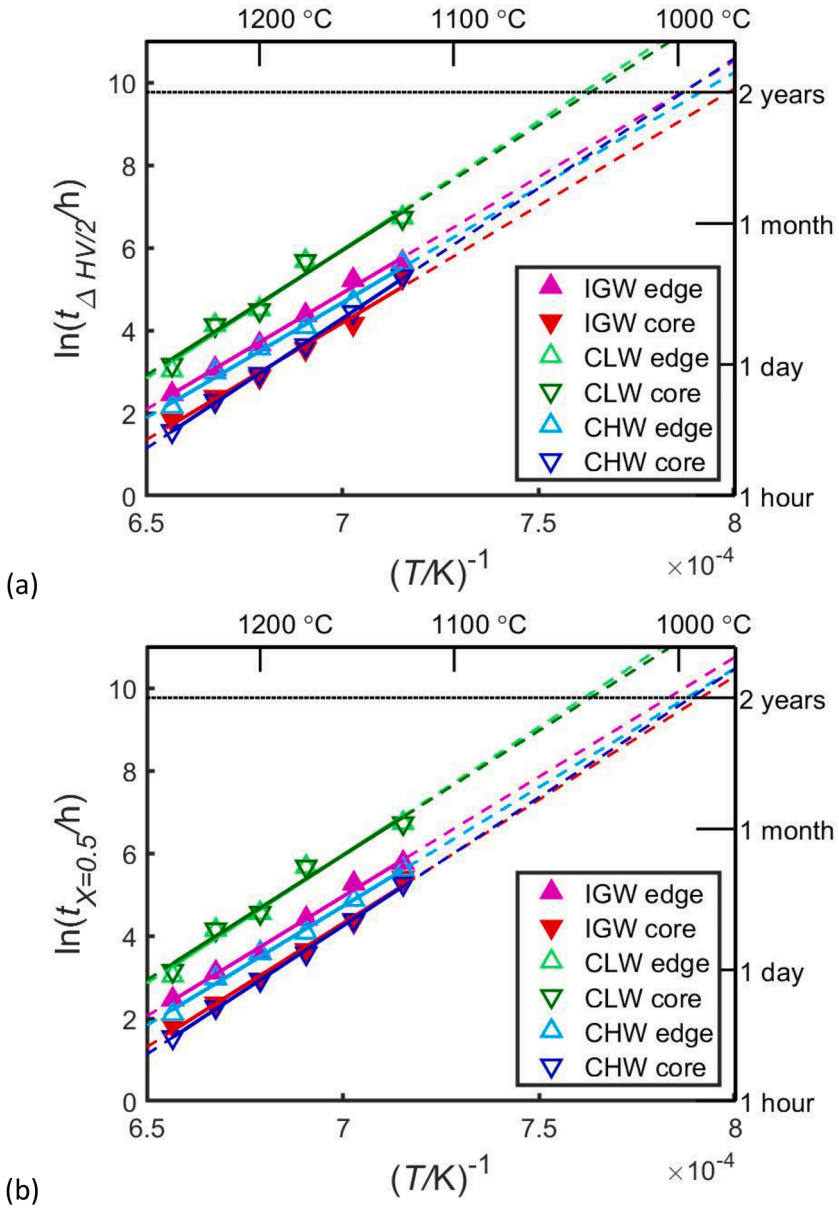

Fig. 5. Arrhenius plots for characteristic restoration times of different regions (core and edge) in three differently rolled tungsten plates received from A.L.M.T., IGW, CLW, and CHW: (a) time to half hardness loss and (b) time to half recrystallization. Plotting the logarithm of characteristic times against the inverse of the absolute temperature presents thermal activated processes following an Arrhenius behavior with constant activation energy as straight lines.

nuclei in a combined manner. All three kinetic parameters are obtained by fitting of the experimental hardness data.

An initial (preliminary) analysis of the recrystallization kinetics without incorporation of any incubation revealed that good fits are obtained with Avrami exponents close to 2. Consequently, the Avrami exponent n was fixed to 2 for all investigated cases. The dashed lines in Figs. 2–4 illustrate the obtained fits of the combined hardness evolution to the experimental data. Fitting the recrystallization kinetics of Eq. (2) allowed obtaining the rate coefficient b, the incubation time t_{inc} and the time to half recrystallization

$$t_{X=0.5} = b^{-1}(\ln 2)^{1/n} + t_{inc} \tag{3}$$

for each temperature for both regions in each of the plates.

Arrhenius plots displaying the logarithm of the characteristic time in dependence on the inverse of the absolute temperature illustrate in Fig. 5 the temperature dependence of both characteristic times. Both, loss of half of the hardness and recrystallization in half of the volume, occur much later in the CLW plate than in the two others. No significant difference between the two different regions in CLW is recognized. This is entirely different for the two other plates, IGW and CHW. Their kinetics is much faster and half hardness loss and half recrystallization are attained much earlier than in CLW. Both plates, IGW and CHW, show quite similar restoration behavior. They display a pronounced heterogeneity with the core undergoing restoration much ahead of the edge regions. Restoration in the cores of both plates occurs on the same time scale, whereas restoration of the edge regions is delayed by a factor of 2 in time in case of IGW and 1.7 for CHW.

4.2. Thermal activation and activation energies

Both characteristic times decrease with increasing annealing temperature T in an Arrhenius manner for thermally activated processes (cf. [15])

$$t = t^{*}\exp\left(\frac{Q}{RT}\right) \tag{4}$$

governed by a constant characteristic activation energy Q with the general gas constant R and a specific, structure-dependent pre-factor t^{*}. Eq. (4) provides a good description of the experimental data from all plates as evident from the fit of straight lines in Fig. 5.

Table 1 lists the activation energies Q obtained by fitting for both characteristic times for the two regions in each plate. The values for the activation energies of the time to half hardness loss are in general similar to or slightly smaller than the ones for the time to recrystallization.

The obtained activation energies characterize the underlying thermally activated physical processes (and are not determined by individual structural features as erroneously stated in [4]). The activation energies for the elementary restoration processes are expected to be comparable to either that of bulk self-diffusion in polycrystalline tungsten (502–586 kJ/mol [3]) or that of short-circuit diffusion (377–460 kJ/mol) [3]. Obviously, the obtained values on the differently rolled tungsten plates summarized in Table 1 often do not correspond to either one of them, but fall in the range between the two intervals. This is rationalized recalling that the reported activation energies are characterizing either losing hardness or the progress of recrystallization in an overall manner. The time to half recrystallization is actually not a result of a single thermally activated process, but rather a combination of three different thermally activated processes [15]: incubation, nucleation and growth of recrystallized grains are not necessarily governed by the same activation energy. The combined effect of the individual processes following different time scales on the time to half recrystallization following from Eq. (3) can lead to activation energies of half recrystallization between the ranges of both types of diffusion slightly deviating from each other (Note, that the rate coefficient b describes nucleation and growth in a combined manner). For the time to half hardness loss, the decaying activation energy of the recovery process [16] leads to even further changes.

Previously (cf. [15]), a general trend has been reported for pure tungsten plates rolled to different thickness reductions (either from AT&M Co. Ltd., China, [4–6] or Plansee SE, Austria, [7,8]) that the apparent activation energies become lower for larger thickness reductions, i.e. larger plastic deformation by warm-rolling. In this manner, the slightly larger activation energy for CLW compared to IGW may indicate a smaller amount of deformation or an intermediate annealing between rolling passes.

4.3. Thermal stability and expected lifetimes

The thermally activated restoration kinetics can be extrapolated to slightly lower temperatures assuming the same thermally activated processes to occur in the very same manner as quantified in the temperature range between 1125 °C and 1250 °C. In this manner, the maximal operation temperature for the armor of a divertor is estimated for which restoration in the tungsten plate does not proceed to half hardness loss or half recrystallization before two full power years in a fusion reactor; table 1 summarizes the predicted values.

The two plates IGW and CHW will just sustain operation temperatures less than 1000 °C for 2 fpy without losing half of the hardness. At higher temperatures, more than half of the hardness will be lost after 2 fpy. Slightly higher operation temperatures less than about 1005 °C will prevent half recrystallization to occur during the same period, recrystallization will proceed to volume fractions higher than 50% above this temperature.

When performing additional investigations for instance on the effect of plasma interaction or irradiation on the restoration kinetics, it is important to take the pronounced heterogeneity between edge and core regions in both plates, IGW and CHW, into account. For their application as monoblocks in a divertor of a fusion reactor (monoblocks are cut with the normal direction of the plasma-facing surface along the rolling direction, cf. [18]), the slightly better thermal stability of the edges compared to the core may actually be beneficial if the edges will receive higher heat fluxes and develop higher temperatures. The slower recrystallization kinetics of the edges of CHW in the investigated temperature interval, however, is compensated partially by the lower activation energy in the edge regions such that the temperatures at which half recrystallization will occur after 2 fpy are almost the same in the edge regions as in the core.

The CLW plate shows in general a delayed restoration by a factor larger than 5 in time compared to the cores of the two other plates, IGW and CHW. CLW shows slightly higher activation energies and even a slightly lower macro hardness in the as-received condition. This indicates that the CLW plate has undergone slightly less plastic deformation than the other two plates or experienced an intermediate anneal during processing causing recovery or post-dynamic recrystallization partially removing the acquired work-hardening. This suspicion has to be further substantiated by microstructural investigations.

The thermal stability of CLW is slightly better than that of IGW and CHW with possible operation temperatures about 1035 °C before recrystallization of half of the volume is expected after 2 fpy. Nevertheless, all plates investigated here are thermally less stable than plates examined earlier by the same method (W67 from AT&M sustains 1075 °C [9], TP1 and TP2 from Plansee 1099 °C and 1088 °C, respectively [13], cf. [15]).

5. Conclusion

The thermal stability of three differently rolled tungsten plates received from A.L.M.T. are investigated thoroughly and their restoration kinetics quantified. The unidirectionally rolled IGW plate and the cross-rolled CHW plate behave rather similar with a pronounced through-thickness heterogeneity of the restoration kinetics between the edge

regions closest to the rolls during rolling and the core of the plates. For both plates, the edge regions show retarded restoration compared to their cores. Extrapolation of their kinetics to even lower temperatures reveals that half recrystallization after two full power years will occur already at temperatures just below 1005 °C. The other cross-rolled plate CLW showed a homogeneous restoration behavior and half recrystallization after 2 fpy is expected only for temperatures slightly above 1035 °C. In this manner, the CLW plate is considered thermally more stable, but still does not surpass the thermal stability of earlier investigated warm-rolled tungsten plates.

Data availability

Datasets related to this article will be made available through EDDI.

CRediT authorship contribution statement

Thomas Larsen: Investigation, Software, Writing – review & editing. **Kevin Chmelar:** Investigation, Software, Writing – review & editing. **Benjamin Lindegren Larsen:** Investigation, Writing – review & editing. **Patrik Nagy:** Investigation, Software, Writing – review & editing. **Kang Wang:** Investigation, Software, Writing – review & editing, Supervision. **Wolfgang Pantleon:** Conceptualization, Data curation, Formal analysis, Writing – original draft, Writing – review & editing, Visualization, Supervision, Project administration, Funding acquisition.

Declaration of Competing Interest

The authors declare that they have no known competing financial interests or personal relationships that could have appeared to influence the work reported in this paper.

Data availability

Data will be made available on request.

Acknowledgement

The authors gratefully acknowledge practical assistance by Lars Lorentzen, Jens Andersen and Zhihao Pan. Kang Wang acknowledges the support from the China Scholarship Council, National MCF Energy R&D program (Grant No. 2019YFE0312003). This work has been carried out within the framework of the EUROfusion Consortium, funded by the European Union via the Euratom Research and Training Programme (Grant Agreement No 101052200 – EUROfusion). Views and opinions expressed are however those of the authors only and do not necessarily reflect those of the European Union or the European Commission. Neither the European Union nor the European Commission can be held responsible for them.

References

[1] R.A. Pitts, et al., J. Nucl.Mater. 438 (2013) S48.
[2] G. Pintsuk, et al., Fusion Eng Des 174 (2022), 112994.
[3] E. Lassner, W.-.D. Schubert, Tungsten; Properties, Chemistry, Technology of the Element, Alloys an Chemical Compounds, Kluwer Academic, New York, 1999, p. 32.
[4] G. Pintsuk, A. Hasegawa, Tungsten as plasma-facing material. Comprehensive Nuclear Materials, Elsevier, 2020, p. 19. Second edition.
[5] P. Schade, Int. J. Refr. Met. Hard Mater. 20 (2002) 301.
[6] J. Reiser, et al., Int. J. Refr. Met. Hard Mater. 54 (2016) 351.
[7] P. Lied, et al., J. Nucl. Mater. 544 (2021), 152664.
[8] J.-.H. Yu, H. Tanigawa, D. Hamaguchi, T. Nozawa, Fusion Eng. Des. 157 (2020), 111679.
[9] A. Alfonso, D. Juul Jensen, G.-.N. Luo, W. Pantleon, J. Nucl. Mater. 455 (2014) 591.
[10] A. Alfonso, D. Juul Jensen, G.-.N. Luo, W. Pantleon, Fusion Eng. Des. 98-99 (2015) 1924.
[11] U.M. Ciucani, W. Pantleon, Fusion Eng. Des. 146 (2019) 814.
[12] U.M. Ciucani, A. Thum, C. Devos, W. Pantleon, Nucl. Mater. Energy 15 (2018) 128.
[13] U.M. Ciucani, A. Thum, C. Devos, W. Pantleon, Nucl. Mater. Energy 20 (2019), 100701.
[14] ASTM E92-17, Standard Test Methods For Vickers Hardness and Knoop Hardness of Metallic Materials, ASTM International, 2017.
[15] W. Pantleon, Phys. Scr. 96 (2021), 124036.
[16] D. Kuhlmann, Z. Phys 124 (1948) 468.
[17] A.N. Kolmogorov, Bull. Acad. Sci. USSR Ser. Math. 3 (1937) 355.
[18] J.H. You, et al., J. Nucl. Mater. 544 (2021), 152670.